

## Preparation of $[\text{Fe}(\text{paptH})_2](\text{CF}_3\text{SO}_3)_2$ and $[\text{Fe}(\text{paptH})_2][\text{Fe}(\text{CN})_5\text{NO}]$ (paptH = bis(2-(pyridin-2-ylamino)-4-(pyridin-2-yl)thiazole): Magnetic, Mössbauer, and Electronic Spectral Properties

Kristian Handoyo Sugiyarto<sup>1\*</sup>, Harold Andrew Goodwin<sup>2</sup>

<sup>1</sup>Department of Chemistry Education, Universitas Negeri Yogyakarta, Yogyakarta 55281, Indonesia

<sup>2</sup>The School of Chemistry, University of New South Wales, Australia

\*Corresponding author email: [sugiyarto@uny.ac.id](mailto:sugiyarto@uny.ac.id)

Received September 02, 2022; Accepted September 28, 2022; Available online November 20, 2022

**ABSTRACT.** Complexes of  $[\text{Fe}(\text{paptH})_2](\text{CF}_3\text{SO}_3)_2 \cdot 1.5\text{H}_2\text{O}$ , and  $[\text{Fe}(\text{paptH})_2][\text{Fe}(\text{CN})_5\text{NO}] \cdot 3\text{H}_2\text{O}$  (paptH = 2-(pyridin-2-ylamino)-4-(pyridin-2-yl)-thiazole, have been characterized in magnetic, Mössbauer, and electronic spectral properties. The studies reveal that the two complexes are predominantly quintet state at room temperature, but singlet at low temperature (below 91K). The change is assigned as a thermally spin state transition, singlet  $^1A_{1g}$  (LS, low-spin)  $\leftrightarrow$  quintet  $^5T_{2g}$  (HS, high-spin), in iron(II), being gradual, continuous, and incomplete at the experimental temperature range, and without hysteresis in these instances. The two complexes were yellowish brown at room temperature ( $\sim 298\text{K}$ ) but darkening to reddish brown at the lower temperatures.

**Keywords:** iron(II), nitroprusside, paptH, spin state transition, triflate

### INTRODUCTION

The chemistry of six coordinated iron(II) with N-donor atom ligand,  $[\text{FeN}_6]^{2+}$ , is of interest to many researchers associated with spin crossover (SCO) system,  $\text{Fe}^{2+}$  (LS;  $\text{singlet-}^1A_1$ ;  $S=0$ )  $\leftrightarrow$   $\text{Fe}^{2+}$  (HS;  $\text{quintet-}^5T_2$ ;  $S=2$ ). Indeed, enormous solid samples have been characterized on finding abrupt-discontinue-with hysteresis samples which are potentially suitable for fundamental and applied aspects in switching electronic devices (Gütlich & Goodwin, 2004; Halcrow, 2013).

The family of bis-tridentate ligand, 3-bpp (2,6-bis(pyridin-3-yl)pyrazole), of iron(II) complexes have been demonstrated to show various types of spin-state transitions depending upon the counter anions for the solid state. While the discontinuous abrupt transition with considerably large hysteresis was observed in the triflate salt (Buchen *et al.*, 1996; Sugiyarto *et al.*, 1997), the abrupt but no hysteresis was observed in the thiocyanate and the nitroprusside salts (Bhattacharjee *et al.*, 2006). The communication of switching spin states can be structurally described (Sugiyarto *et al.*, 2003). Quite recently, the effect of

trifluoro acetate (TFA) anion has been also structurally determined (Sugiyarto *et al.*, 2021).

Another family of a tridentate ligand of paptH [2-(pyridin-2-ylamino)-4-(pyridin-2-yl)] (Figure 1) of iron(II) complexes might also be of interest. Among others of various anionic salts, for the nitrate salt, the continuous spin-state transition is associated with a marked thermal hysteresis. This complex is very unusual, since hysteresis is commonly observed for the abrupt-discontinuous transition. Moreover, the high-spin fraction in the nitrate salt can be trapped at low temperatures by rapid cooling method and the kinetics of  $\text{Fe}^{2+}$  ( $\text{quintet-}^5T_2$ )  $\rightarrow$   $\text{Fe}^{2+}$  ( $\text{singlet-}^1A_1$ ) transformation was then studied [Ritter *et al.*, 1978], as also described in  $[\text{Fe}(3\text{-bpp})_2](\text{BF}_4)_2$  and  $[\text{Fe}(3\text{-bpp})_2](\text{CF}_3\text{CSO}_3)_2$  (Bunchen *et al.*, 1996; Sugiyarto *et al.*, 1997), but for abrupt-discontinuous spin-state transition. The coordination mode of paptH in the crystal of  $\text{Fe}(\text{paptH})_2[\text{BF}_4]_2 \cdot 3\text{H}_2\text{O}$  was also structurally determined and found to act as tridentate via N(1) - N(3) - N(4) (Figure 1), with bond length of high-spin state- $^5T_2$  of iron(II) (König *et al.*, 1983).

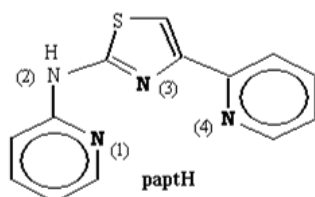


Figure 1. 2-(pyridin-2-ylamino)-4-(pyridin-2-yl)-thiazole (paptH)

Because of the relative "unique" nature of iron(II) in  $[\text{Fe}(\text{paptH})_2][\text{NO}_3]_2$ , the work was extended to the other corresponding triflate,  $\text{CF}_3\text{SO}_3^-$ , and nitroprusside,  $[\text{Fe}(\text{CN})_5\text{NO}]^{2-}$  salts. This would give at least more information about the anionic effects in the spin state transition of iron(II) system for this ligand.

## MATERIALS AND METHODS

### Materials

The main common chemicals, 2-( $\omega$ )-bromoacetylpyridine, 2-pyridylthiourea,  $\text{Na}_2\text{CO}_3$ , HBr,  $\text{FeCl}_2 \cdot 4\text{H}_2\text{O}$ ,  $\text{LiCF}_3\text{SO}_3$  or  $\text{Na}_2[\text{Fe}(\text{CN})_5\text{NO}]$ , were purchased from Aldrich and used as they are received.

### Preparation of Ligand

The free ligand paptH ( $\text{C}_{13}\text{H}_{10}\text{N}_4\text{S}$ ) was prepared in two steps. The first was the preparation of 2-bromoacetylpyridine according to a method adapted from Clemo *et al.* (1937), and the second was the preparation of paptH based on the general reaction of thiourea as described by Sylva and Goodwin (1967). A solution of 2-( $\omega$ )-bromoacetylpyridine (2 g) in ether (25 mL) was added to a solution of 2-pyridylthiourea (1.53 g) in ethanol (5 mL). The mixture became cloudy and then, the pale yellow thiazole hydrobromide was precipitated. This was allowed to stand for about 30 minutes and then ether (~ 100 mL) was added to complete the reaction. The solid was filtered, dissolved in hot water (~ 30 mL) and a small amount of HBr. The free thiazole was separated after the solution was basified with  $\text{Na}_2\text{CO}_3$ . It was filtered, and recrystallized from ethanol to give creamy white needle-shaped crystals. The melting point of 204 - 206 °C for this compound is in line with that found in the literature (Sylva & Goodwin, 1967). The elemental analysis was found to be C, 60.9 %; H, 3.9 %; N, 21.6% (Calculated for  $\text{C}_{13}\text{H}_{10}\text{N}_4\text{S}$ : C, 61.4 %; H, 4.0% ; N, 22.0 %). The analysis is also supported by the  $^1\text{H}$ -NMR spectrum. The proton resonance arising at 6.9 - 8.6 ppm and ~ 11.5 ppm correspond to the pyridine- and thiazole-, and imine NH- hydrogen atoms; the relative integral values are consistent with this assignment.

### Preparation of Complexes

The complexes of  $[\text{Fe}(\text{paptH})_2](\text{CF}_3\text{SO}_3)_2$  and  $[\text{Fe}(\text{paptH})_2][\text{Fe}(\text{CN})_5\text{NO}]$  were prepared as follows. To a warmed ethanolic solution of paptH (2 mmol, ~ 4 mL) was added an aqueous solution of  $\text{FeCl}_2 \cdot 4\text{H}_2\text{O}$  (1 mmol, ~ 3 mL). The mixture was filtered and the aqueous solution of either  $\text{LiCF}_3\text{SO}_3$  or  $\text{Na}_2[\text{Fe}(\text{CN})_5\text{NO}]$  in slight excess (3 mmol, ~ 3 mL) was added where upon the yellowish brown precipitate was resulted on scratching. The precipitate was filtered, washed with cold water and then dried in air. For the preparation of  $^{57}\text{Fe}(\text{paptH})_2[\text{Fe}(\text{CN})_5\text{NO}]$ , the aqueous solution of precursor iron(II) chloride was first prepared from the reaction of a mixture of  $^{57}\text{Fe}$  and  $^{56}\text{Fe}$  in the mass ratio of 60:40 with

hydrochloric acid. All reactions were carried out in a nitrogen atmosphere. The two complexes were isolated as the corresponding triflate sesquihydrate,  $[\text{Fe}(\text{paptH})_2][\text{CF}_3\text{SO}_3]_2 \cdot 1.5\text{H}_2\text{O}$ , and the nitroprusside trihydrate,  $[\text{Fe}(\text{paptH})_2][\text{Fe}(\text{CN})_5\text{NO}] \cdot 3\text{H}_2\text{O}$ . The C, H, and N elemental analysis results are as follows, Found: C, 37.92 %; H, 2.75 %; N, 12.60 %; calculated for  $[\text{Fe}(\text{paptH})_2][\text{CF}_3\text{SO}_3]_2 \cdot 1.5\text{H}_2\text{O}$ : C, 37.80 %; H, 2.61 %; N, 12.60 %. Found: C, 44.93 %; H, 3.16 %; N, 23.26 %; calculated for  $[\text{Fe}(\text{paptH})_2][\text{Fe}(\text{CN})_5\text{NO}] \cdot 3\text{H}_2\text{O}$ : C, 44.62 %; H, 3.14 %; N, 23.50 %. Each of the two complexes was prepared in two samples, sample 1 and sample 2, to confirm the reproducibility of the magnetic property for each complex.

### Physical Measurements

**Magnetism.** The magnetic susceptibility was recorded using a Newport variable temperature Gouy balance calibrated with  $\text{CoHg}(\text{NCS})_4$ . All data were corrected for diamagnetism calculated by using Pascal's constants (Bain & Berry, 2008). The relationship of  $\mu_{\text{eff}} = 2.828 \sqrt{\chi'_M T}$  BM, where  $\chi'_M$  = the corrected molar susceptibility, and  $T$  = temperature of the sample, was applied to the calculation of effective magnetic moment (Dalal, 2017; Pathshala, 2021; LibreTexts™, 2021; Lancashire, 2021).

**Mössbauer and Electronic Spectra.** The Mössbauer spectra were recorded in a constant acceleration spectrometer in a transmission mode of a  $^{57}\text{Co}$  source in a palladium matrix at room temperature, a Wissel drive unit, and a Norland multichannel analyser. For measurement at low temperature (~ 80 K), the sample was placed in a special holder contacted with liquid nitrogen. The instrument was calibrated with metallic iron foil and sodium nitroprusside, and the isomer shift values are quoted relative to the midpoint of the sodium nitroprusside spectrum at room temperature. The spectral parameters were calculated from a least squares fit of the experimental data to Lorentzian line shapes. To get a strong resolution, the sample was enriched with  $^{57}\text{Fe}$  to about 60 % for the cationic site.

A spectrophotometer of Zeiss PMQII equipped with an accessory for diffuse reflectance spectral recording was employed as described in Sugiyarto *et al.* (1995). The powder samples mixed with magnesium oxide for calibration were spread on a filter paper for recording the spectra, and a special brass contacting with a brass dewar containing liquid nitrogen was applied for low-temperature measurements.

## RESULTS AND DISCUSSION

### Magnetism

The magnetism of  $[\text{Fe}(\text{paptH})_2](\text{CF}_3\text{SO}_3)_2 \cdot 1.5\text{H}_2\text{O}$ , and  $[\text{Fe}(\text{paptH})_2][\text{Fe}(\text{CN})_5\text{NO}] \cdot 3\text{H}_2\text{O}$  have been measured in the range 91-302K for both decreasing- and increasing- temperature sequences. The effective

magnetic moment,  $\mu_{\text{eff}}$  for the triflate (sample 1) at 302K and 383K are 5.01 BM and 5.23 BM, respectively. This is indicative of a predominantly high-spin  $^5T_{2g}$  ground state with a small fraction of low-spin  $^1A_{1g}$  at room temperature. At 91K, however,  $\mu_{\text{eff}}$  of about 2.18 BM implies a predominantly low-spin  $^1A_{1g}$  ground state with a small fraction of high-spin,  $^5T_{2g}$ . The change in a moment due to temperature change is gradual (**Figure 2**), and reversible as shown in data collected according to the order of measurements (**Table 1**). The reproducibility of the magnetic change for this salt was confirmed by the magnetic data (**Figure 2, Table 1**) for sample 2 which was separately prepared from sample 1.

A quite similar variation in magnetism was also observed for the nitroprusside trihydrate (**Figure 2, Table 1**). The magnetic moment values for this salt at the same temperatures as for the triflate salt, however, are always slightly lower. These, for example, are 4.23 BM at 313K and 4.74 BM at 373K for the nitroprusside trihydrate (sample 2, **Table 1**), but 5.10 BM at 313K and 5.22 BM at 373K for the triflate (sample 2, **Table 1**). Thus, the change in magnetism for the two complexes is associated with thermally spin state transition, singlet  $^1A_{1g}$  (LS)  $\leftrightarrow$  quintet  $^5T_{2g}$  (HS), in iron(II). The transition is gradual, incomplete, and no hysteresis was observed in these instances similar to the other anionic salts (Sylva & Goodwin, 1967).

#### Mössbauer Effect

Confirmation of the virtually spin-state transition in  $[\text{Fe}(\text{paptH})_2]^{2+}$  was clearly demonstrated by

measurements of Mössbauer spectroscopy (Sugiyarto *et al.*, 2003; Sugiyarto *et al.*, 2021; Ritter *et al.*, 1978). In this work, the study of Mössbauer spectra for the nitroprusside salt,  $[\text{Fe}(\text{paptH})_2][\text{Fe}(\text{NO})_5\text{NO}] \cdot 3\text{H}_2\text{O}$ , was considered desirable, since the nitroprusside anion containing iron(II) would also display clearly the two typical lines of singlet state. For this reason, a sample containing  $[\text{Fe}(\text{paptH})_2]^{2+}$  cation enriched with  $\sim 60\%$   $^{57}\text{Fe}$  was prepared. The spectrum was then recorded for sodium nitroprusside (as a reference), for the salt containing natural iron (Sample 1), and for the  $^{57}\text{Fe}$  enriched sample (Sample 2). The spectra are shown in **Figure 3** and their detailed parameters are listed in **Table 2**. As expected, the spectrum of sodium nitroprusside (at room temperature) reveals a typical doublet containing the two lines of low-spin iron(II) in the anionic site. The spectrum for the natural sample (Sample 1) reveals strongly four lines. The main four lines were well assigned to two doublets, doublet I and doublet II.

It is clear from **Figure 3B** that doublet I certainly corresponds to low-spin iron(II) in the nitroprusside anion (Sugiyarto *et al.*, 2003). Doublet II is then due to the iron(II) cationic site; its parameters, quadrupole splitting,  $\Delta E_Q = 2.37 \text{ mm s}^{-1}$ , and isomer shift,  $\delta_{\text{IS}} = 1.23 \text{ mm s}^{-1}$ , are assigned as high-spin iron(II) (Sugiyarto *et al.*, 2021). Somewhat asymmetric of the doublet is diagnostic, and it is presumably associated with the presence of a very small fraction of singlet state iron(II), as indicated by the room temperature magnetic moment.

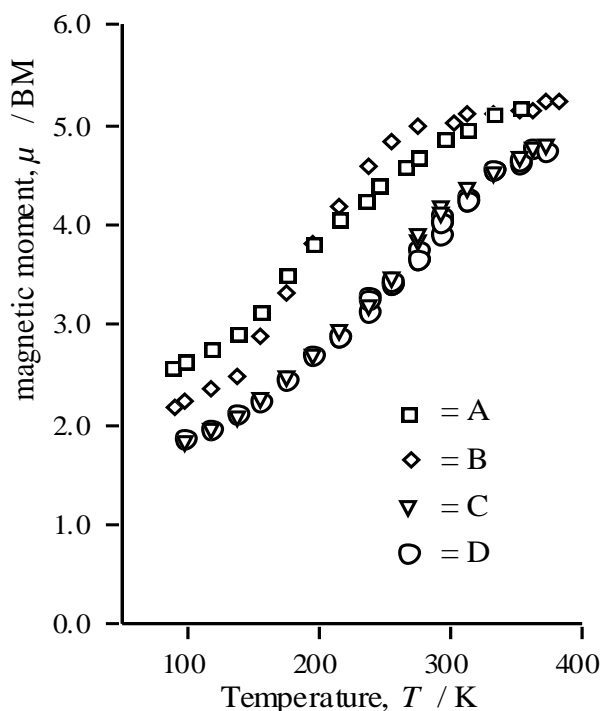


**Figure 2.** Magnetic Moment,  $\mu$ , versus Temperature,  $T$  for:  $[\text{Fe}(\text{paptH})_2][\text{CF}_3\text{SO}_3]_2 \cdot 1.5\text{H}_2\text{O}$  -Sample 1 (A) and Sample 2 (B),  $[\text{Fe}(\text{paptH})_2][\text{Fe}(\text{CN})_5(\text{NO})] \cdot 3\text{H}_2\text{O}$  -Sample 1 (C) and Sample 2 (D)

**Table 1.** Magnetic data of complexes

[Fe(papthH) <sub>2</sub> ][Fe(CN) <sub>5</sub> NO]·3H <sub>2</sub> O (Sample 1)			[Fe(papthH) <sub>2</sub> ][CF <sub>3</sub> SO <sub>3</sub> ] <sub>2</sub> ·1.5 H <sub>2</sub> O					
			Sample 1			Sample 2		
T/K	$\chi_M / 10^{-6}$	$\mu_{\text{eff}} / \text{BM}$	T/K	$\chi_M / 10^{-6}$	$\mu_{\text{eff}} / \text{BM}$	T/K	$\chi_M / 10^{-6}$	$\mu_{\text{eff}} / \text{BM}$
293.3	7380	4.16	295	9993	4.85	303.2	10358	5.01
215.6	4880	2.90	265	9993	4.60	237.2	11164	4.60
156.5	4004	2.24	235.2	9624	4.25	176.3	7807	3.32
98.9	4046	1.79	196	9274	3.81	91	6532	2.18
118.1	3921	1.92	156.5	7837	3.13	99	6297	2.23
137.2	3838	2.05	118	8022	2.75	118.1	5827	2.35
176.3	4296	2.46	89	9439	2.59	137.2	5592	2.48
195.8	4588	2.68	98.9	8782	2.63	156.5	6599	2.87
237.2	5255	3.16	137.2	7775	2.92	195.8	9251	3.81
255	5838	3.45	176.3	8658	3.49	215.6	10156	4.18
275	6630	3.82	215.6	9624	4.07	255	11432	4.83
313.2	7547	4.35	244.9	9870	4.40	275	11298	4.98
293.3	7172	4.10	275	9932	4.67	313.2	10392	5.10
275	6797	3.87	313.2	9788	4.95	333.2	9788	5.11
333.2	7566	4.49	333.2	9747	5.10	353.2	9318	5.13
353.2	7631	4.64	353.2	9418	5.16	363.2	9083	5.14
363.2	7756	4.75				373.2	9150	5.22
373.2	7589	4.76				383.2	8948	5.23

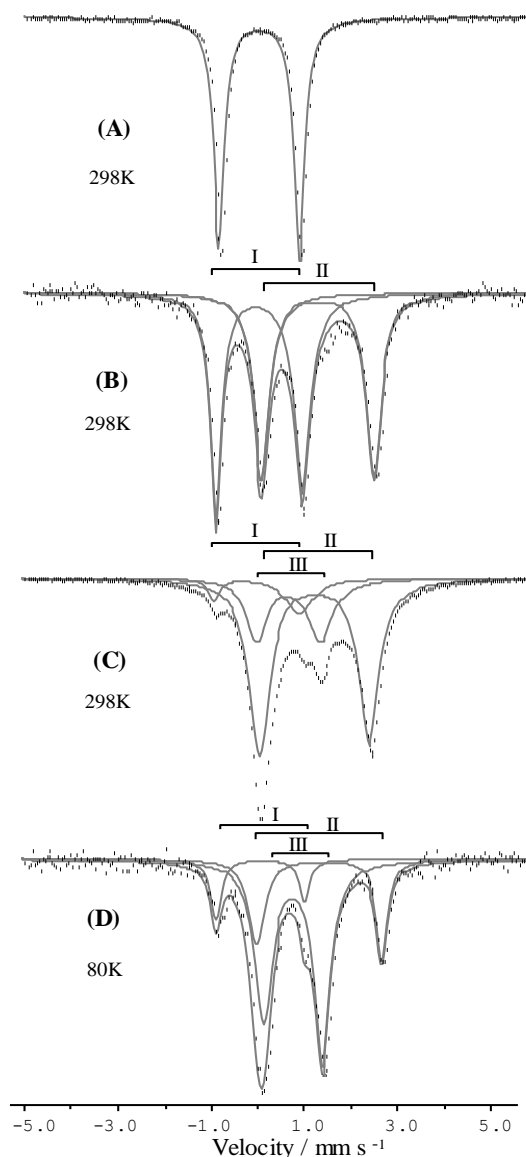
  

[ <sup>57</sup> Fe(papthH) <sub>2</sub> ][Fe(CN) <sub>5</sub> NO]·3H <sub>2</sub> O (Sample 2)								
T/K	$\chi_M / 10^{-6}$	$\mu_{\text{eff}} / \text{BM}$	T/K	$\chi_M / 10^{-6}$	$\mu_{\text{eff}} / \text{BM}$	T/K	$\chi_M / 10^{-6}$	$\mu_{\text{eff}} / \text{BM}$
293.3	7147	4.09	293.3	6515	3.91	313.2	7333	4.29
215.6	4806	2.88	313.2	7147	4.23	333.2	7816	4.56
156.5	3988	2.23	293.3	6962	4.04	353.2	7594	4.63
98.9	4397	1.86	275	6441	3.76	363.2	7816	4.76
118.1	4062	1.96	255	5661	3.40	373.2	7519	4.74
137.2	4025	2.10	237.2	5215	3.14	353.2	7705	4.66
176.3	4248	2.45	215.6	4806	2.88	333.2	7779	4.55
195.8	4620	2.69	237.2	5586	3.26	313.2	7185	4.24
237.2	5735	3.30	255	5772	3.43	293.2	6962	4.04
255	5735	3.42	275	6144	3.67			
275	6107	3.66	293.2	7036	4.06			

The effect of temperature on the spectra of [<sup>57</sup>Fe(papthH)<sub>2</sub>][Fe(CN)<sub>5</sub>NO] is clearly shown in **Figures 3C** (at 298K) and **2D** (at 80K). In this case, each spectrum may be resolved into three doublets, doublet I, II, and III. Doublet I is clearly assigned to the low-spin state of iron(II) in nitroprusside anion, whereas doublet II and doublet III should correspond to the high-spin iron(II) cation and the low-spin one, respectively. At room temperature, doublet II is much more dominant than doublet III, but at low temperature doublet III becomes much more dominant than doublet II. This is certainly consistent with the magnetic change.

These Mössbauer spectral parameters are quite similar to those reported for the other salts of

[Fe(papthH)<sub>2</sub>]<sup>2+</sup>, the perchlorate, tetrafluoroborate and nitrate (Koenig *et al.*, 1983; Sylva & Goodwin, 1967), and [Fe(pzapthH)<sub>2</sub>]<sup>2+</sup> (pzapthH = 2-(pyrazin-2-ylamino)-4-(pyridin-2-yl)thiazole) (Childs *et al.*, 1997), and they are typical diagnostic for the spin states of iron(II) as listed in **Table 2**. For the low-spin state, the quadrupole splitting observed seems to be high and is greater than those reported for other salts of tridentate [Fe(3-bpp)<sub>2</sub>]<sup>2+</sup> (Sugiyarto *et al.*, 1997). It is presumably associated with the possible distortion which may be inherent in the coordination of the meridional tridentate system, but it is more pronounced in this complex due to the asymmetrical configuration of the ligand system (Childs *et al.*, 1997).



**Figure 3** Mössbauer Spectra of  $\text{Na}_2[\text{Fe}(\text{CN})_5\text{NO}]$  at  $\sim 298\text{K}$  (A),  $[\text{Fe}(\text{papthH})_2][\text{Fe}(\text{CN})_5\text{NO}] \cdot 3\text{H}_2\text{O}$  at  $\sim 298\text{K}$  (B), and  $^{57}\text{Fe}(\text{papthH})_2[\text{Fe}(\text{CN})_5\text{NO}] \cdot 3\text{H}_2\text{O}$  at  $\sim 298\text{K}$  (C) and  $\sim 80\text{K}$  (D)

**Table 2.** Mössbauer spectral parameters for iron(II) complexes

	Iron(II) complexes	$\Delta E_Q /$ $\text{mm s}^{-1}$	$\delta_{\text{is}} /$ $\text{mm s}^{-1}$	Spin State	
(A).	$\text{Na}_2[\text{Fe}(\text{CN})_5\text{NO}]$ (298K)	1.70	0 (ref.)	$^1\text{A}_{1g}$ (LS) $[\text{Fe}(\text{CN})_5\text{NO}]^{2-}$	
(B).	$[\text{Fe}(\text{papthH})_2][\text{Fe}(\text{CN})_5\text{NO}] \cdot 3\text{H}_2\text{O}$ (298K) : doublet I	1.82	- 0.03	$^1\text{A}_{1g}$ (LS) $[\text{Fe}(\text{CN})_5\text{NO}]^{2-}$	
		doublet II	2.37	1.23	$^5\text{T}_{2g}$ (HS)
(C).	$^{57}\text{Fe}(\text{papthH})_2[\text{Fe}(\text{CN})_5\text{NO}] \cdot 3\text{H}_2\text{O}$ (298K) : doublet I	1.82	- 0.03	$^1\text{A}_{1g}$ (LS) $[\text{Fe}(\text{CN})_5\text{NO}]^{2-}$	
		doublet II	2.29	1.18	$^5\text{T}_{2g}$ (HS)
		doublet III	1.35	0.63	$^1\text{A}_{1g}$ (LS)
(D).	$^{57}\text{Fe}(\text{papthH})_2[\text{Fe}(\text{CN})_5\text{NO}] \cdot 3\text{H}_2\text{O}$ (80K) : doublet I	1.86	0.04	$^1\text{A}_{1g}$ (LS) $[\text{Fe}(\text{CN})_5\text{NO}]^{2-}$	
		doublet II	2.62	1.29	$^5\text{T}_{2g}$ (HS)
		doublet III	1.35	0.63	$^1\text{A}_{1g}$ (LS)

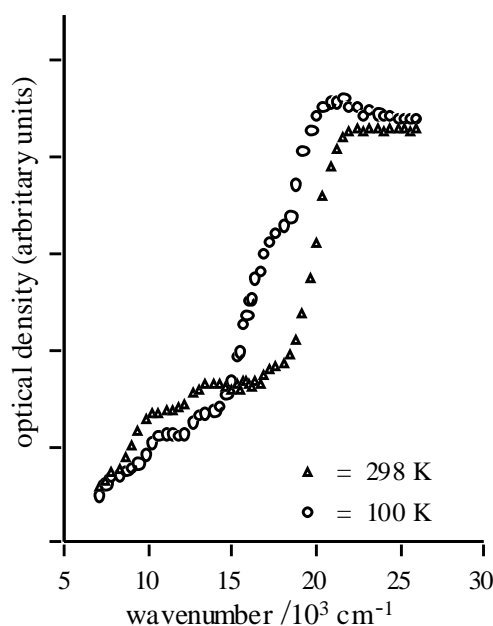


**Figure 4.** Diffuse reflectance spectra for  $[\text{Fe}(\text{paptH})_2][\text{CF}_3\text{SO}_3]_2 \cdot 1.5\text{H}_2\text{O}$  at 298K and 100K

### Electronic Spectra

The electronic spectra for the two complexes are quite similar. They are fairly pronounced temperature-dependent on the spin-state of iron(II) in the solid state. Thus, the diffuse reflectance spectrum of  $[\text{Fe}(\text{paptH})_2][\text{Fe}(\text{CN})_5\text{NO}] \cdot 3\text{H}_2\text{O}$  at room temperature (**Figure 4**), reveals prominent high-spin ligand field absorption split into two, centered at about 10000 and 13000  $\text{cm}^{-1}$ ; this is associated with high-spin state and corresponds to the  ${}^5T_{2g} \rightarrow {}^5E_g$  transition. The splitting arises presumably from Jahn-Teller and/or low-symmetry effects (Lancashire, 2022; Bersuker, 2021; Halcrow, 2013), and this may be due to the "asymmetric" electronic configuration of the metal atom ( $t_2^4 e^2$ ) and/or the different strength in the nitrogen atom coordination of the tridentate-paptH as indicated by the different bond length for the Fe-N(1), Fe-N(3), and Fe-N(4) in  $[\text{Fe}(\text{paptH})_2][\text{BF}_4]_2 \cdot 3\text{H}_2\text{O}$  (König *et al.*, 1983). Strong absorption observed at about 22000  $\text{cm}^{-1}$  seems to be assigned as Metal-Ligand charge-transfer band.

At low temperatures, the intensity of ligand field absorption due to the quintet-state fraction is clearly much reduced, and it is consistent with the reduced population of the high-spin fraction (as reflected by the Mössbauer and magnetic data). A very pronounced shoulder arising at about 18000  $\text{cm}^{-1}$  at low temperature is most likely associated with the low-spin ligand field band, being the origin of the  ${}^1A_{1g} \rightarrow {}^1T_{1g}$  transition in a singlet state iron(II). This is not generally resolved in spin-state transition systems of iron(II) due to its overlap with the absorption of the charge transfer band. However, in the spectrum of  $[\text{Fe}(\text{ptz})_6][\text{BF}_4]_2$  (where ptz = 1-propyltetrazole), for example, it is well resolved at 18400  $\text{cm}^{-1}$  (Decurtins, 1985) and that of

$[\text{Fe}(\text{trzH})_2(\text{trz})][\text{X}]$  (where trzH = 1,2,4-triazole, trz = deprotonated 1,2,4-triazole, and X =  $\text{BF}_4$ ,  $\text{ClO}_4$ , and  $\text{PF}_6$ ) it is at 18800  $\text{cm}^{-1}$  (Sugiyarto *et al.*, 1995; Sugiyarto *et al.*, 1993).

It should also be noted that at low temperatures, the principal charge transfer band is observed to be more intense and is significantly displaced to lower energy, at 20500  $\text{cm}^{-1}$ . Thus, due to the reduced Fe-N bond length at low temperature, the  $t_2(\text{M})$  the  $t_2(\text{M}) \rightarrow \pi^*(\text{ligand})$  charge transfer becomes more facile and consequently lower energy, and this may account for the visible darkening of the complex from yellowish brown at room temperature to reddish brown at low temperature.

Thus, no specific properties associated with hysteresis and/or discontinuous spin state transitions were observed, and these are similar to the previously reported complexes (König *et al.*, 1983; Sylva & Goodwin, 1967), but differ from the corresponding nitrate complex (Ritter *et al.*, 1978). However, these should support that the tridentate ligand, paptH, provides an intermediate ligand field to allow an equilibrium of the singlet  ${}^1A_{1g}$  (low-spin)  $\leftrightarrow$  quintet  ${}^5T_{2g}$  (high-spin) in iron(II). In addition, the thermochromic nature can be significantly demonstrated in accompanying the occurrence of spin crossover in these complexes.

### CONCLUSIONS

$[\text{Fe}(\text{paptH})_2][\text{CF}_3\text{SO}_3] \cdot 1.5\text{H}_2\text{O}$  and  $[\text{Fe}(\text{paptH})_2][\text{Fe}(\text{CN})_5(\text{NO})] \cdot 3\text{H}_2\text{O}$  display a thermally spin state transition, singlet  ${}^1A_{1g} \leftrightarrow$  quintet  ${}^5T_{2g}$ , in iron(II). It is accompanied by thermochromic nature, being yellowish brown at room temperature but reddish brown at lowering temperatures. Within the range of

experimental temperatures, the transition is continuous and incomplete. The complexes are mainly high-spin nature with a minor fraction of low-spin at  $\sim 298$  K, and they are dominantly low-spin with minor residual paramagnet at  $\sim 90$  K. The room-temperature high-spin ligand field band splits at 10000 and 13000  $\text{cm}^{-1}$ , whereas the low-temperature low-spin one arises at about 18000  $\text{cm}^{-1}$ . The room-temperature charge transfer absorption at 22000  $\text{cm}^{-1}$  was observed to be more intense and moves to a lower energy, 20500  $\text{cm}^{-1}$  at  $\sim 100$ K, and this is associated with the thermochromic behaviour in these instances.

## ACKNOWLEDGEMENTS

Kristian gratefully acknowledges support for this work in collecting data provided by Prof. H. A. Goodwin, Department of Inorganic Chemistry, the School of Chemistry, UNSW - AUSTRALIA.

## CONFLICTING OF INTEREST

The authors declare that there is no conflict of interest regarding the publication of this article.

## REFERENCES

- Bain, G. A., & Berry, J. F.. (2008). Diamagnetic corrections and pascal's constants. *Journal of Chemical Education*, 85(4): 532-536. <https://doi.org/10.1021/ed085p532>.
- Bersuker, I. B. (2021). The jahn-teller and pseudo-jahn-teller effects: a unique and only source of spontaneous symmetry breaking in atomic matter. *Symmetry*, 13(1577), 1-10. <https://doi.org/10.3390/sym13091577>.
- Bhattacharjee, A., Kusz, J., Ksenofontov, V., Sugiyarto, K. H., Goodwin, H. A., & Gütllich, P. (2006). X-ray powder diffraction and LIESST-effect of the spin transition material  $[\text{Fe}(\text{3-bpp})_2](\text{NCS})_2 \cdot 2\text{H}_2\text{O}$ . *Chemical Physics Letters*, 431(1-3), 72–77. <https://doi.org/10.1016/j.cplett.2006.09.052>.
- Buchen, T., Gütllich, P., Sugiyarto, K. H., & Goodwin, H. A. (1996). High-spin  $\rightarrow$  low-spin relaxation in  $[\text{Fe}(\text{bpp})_2](\text{CF}_3\text{SO}_3)_2 \cdot \text{H}_2\text{O}$  after LIESST and thermal spin-trapping-dynamics of spin transition versus dynamics of phase transition. *Chemistry European Journal*, 2(9): 1134-1138. <https://doi.org/10.1002/chem.1996002091>.
- Childs, B. J., Cadogan, J. M., Craig, D. C., Scudder, M. L., Goodwin, H. A. (1997). Electronic and structural properties of iron(II) and nickel(II) cationic complexes of 2-(pyrazin-2-ylamino)-4-(pyridin-2-yl)thiazole. *Australian Journal of Chemistry*, 50(2), 129-138. <https://doi.org/10.1071/C96185>.
- Clemo, G. R., Morgan, W. M., & Raper, R. (1937). The lupin alkaloids. Part XII. The synthesis of dl-lupinine and dl-isolupinine. *Journal of the Chemical Society*, 965-969. <https://doi.org/10.1039/jr9370000965>.
- Dalal, M. A. (2017). Textbook of Inorganic Chemistry- Volume 1 (First Edition). CHAPTER 9. *Magnetic properties of transition metal complexes*. India: Dalal Institute, pp.342-386.
- Decurtins, S., Gütllich, P., Hasselbach, K. M., Hauser, A., Spiering, H. (1985). Light-induced excited-spin-state trapping in iron(II) spin-crossover systems. Optical spectroscopic and magnetic susceptibility study. *Inorganic Chemistry*, 24, 2174-2178. <https://doi.org/10.1021/ic00208a013>.
- Gütllich, P., & Goodwin, H. A. (2004). in *Spin Crossover in Transition Metal Compounds I*, Springer: 1-47.
- Halcrow, M. A. (2013) Jahn-Teller distortions in transition metal compounds, and their importance in functional molecular and inorganic materials. *Chemical Society Reviews*, 42(4), 1784-1795. <https://doi.org/10.1039/c2cs35253b>.
- Halcrow, M. A. (2013). *Spin-crossover materials: properties and applications*. John Wiley and Sons.
- Köenig, E., Ritter, G., Kulshreshtha, S. K., & Goodwin, H. A. (1983). Nature of the continuous high-spin ( $^5T_2$ )  $\leftrightarrow$  low-spin ( $^1A_1$ ) transition in bis[2-[(4-methyl-2-pyridyl)amino]-4-(2-pyridyl)thiazole]iron(II) diperchlorate dihydrate and bis(tetrafluoroborate) dihydrate: Mössbauer effect and X-ray diffraction study. *Inorganic Chemistry*, 22(18), 2518–2523. <https://doi.org/10.1021/ic00160a011>.
- Lancashire, R. J. (2020). *LibreTexts™: Magnetic Moments of Transition Metals*. <https://chem.libretexts.org/@go/page/19707> [accessed 15 December 2021].
- Lancashire, R. J. (2021) LibreTexts™: *Jahn-Teller Effect*. <https://chem.libretexts.org/@go/page/188706> [accessed 27 January 2022].
- LibreTexts™ (2020). *Magnetism*. <https://chem.libretexts.org/@go/page/263246>. [accessed 15 December 2021].
- LibreTexts™ (2021). *Magnetic susceptibility and the spin-only formula*. <https://chem.libretexts.org/@go/page/34408>. [accessed 15 December 2021].
- Pathshala (2021). *Inorganic chemistry-II: metal-ligand bonding, electronic spectra and magnetic properties of transition metal complexes*. [http://meerutcollege.org/mcm\\_admin/upload/1588000002.pdf](http://meerutcollege.org/mcm_admin/upload/1588000002.pdf). [accessed 15 December 2021].
- Ritter, G., Köenig, E., Irlner, W., & Goodwin, H. A. (1978). The high-spin( $^5T_2$ )  $\leftrightarrow$  low-spin( $^1A_1$ ) transition in solid bis[2-(2-pyridylamino)-4-(2-pyridyl)thiazole]iron(II) dinitrate. Its dependence on time and on the previous history of the specimen. *Inorganic Chemistry*, 17(2), 224–

228. <https://doi.org/10.1021/ic50180a005>.
- Sugiyarto, K. H., Craig, D. C., Rae, A. D., Goodwin, H. A. (1993). Structural and electronic properties of iron(II) and nickel(II) complexes of 2,6-bis(triazol-3-yl)pyridines. *Australian Journal of Chemistry*, 46, 1269-1290. <https://doi.org/10.1071/CH9931269>.
- Sugiyarto, K. H., Craig, D. C., Rae, A. D., Goodwin, H. A. (1995). Structural and electronic properties of iron(II) complexes of 2-(1,2,4-triazol-3-yl)pyridine and substituted derivatives. *Australian Journal of Chemistry*, 48(1): 35-54. <https://doi.org/10.1071/ch9950035>.
- Sugiyarto, K. H., McHale, W. A., Craig, D. C., Rae, A. D., Scudder, M. L., & Goodwin, H. A. (2003). Spin transition centres linked by the nitroprusside ion. The cooperative transition in bis(2,6-bis(pyrazol-3-yl)pyridine)iron(II) nitroprusside. *Dalton Transactions*, 12, 2443-2448. <https://doi.org/10.1039/b301218b>.
- Sugiyarto, K. H., Onggo, D., Akutsu, H., Reddy, V. R., Sutrisno, H., Nakazawa, Y., & Bhattacharje, A. (2021). Structural, magnetic and Mössbauer spectroscopic studies of the [Fe(3-bpp)<sub>2</sub>](CF<sub>3</sub>COO)<sub>2</sub> complex: role of crystal packing leading to an incomplete Fe(II) high spin ↔ low spin transition, *CrystEngComm*, 23, 2854-2861. <https://doi.org/10.1039/d0ce01687j>.
- Sugiyarto, K. H., Weitzner, K., Craig, D. C., & Goodwin, H. A. (1997). Structural, magnetic and mössbauer studies of bis(2,6-bis(pyrazol-3-yl)pyridine)iron(II) triflate and its hydrates. *Australian Journal of Chemistry*, 50(9): 869-873. <https://doi.org/10.1071/c96206>.
- Sylva, R. N., & Goodwin, H. A. (1967). Anomalous magnetic properties in the solid state of salts of the Bis[2-(2-pyridylamino)-4-(2-pyridyl)thiazole]iron(II) ion. *Australian Journal of Chemistry*, 20, 479-496. <https://doi.org/10.1071/CH9670479>.